Have female twisted-wing parasites (Insecta: Strepsiptera) evolved tolerance traits as response to traumatic penetration?

Kenny Jandausch [Corresp., 1, 2] , **Jan Michels** [3] , **Alexander Kovalev** [3] , **Stanislav N Gorb** [3] , **Thomas van de Kamp** [4, 5] , **Rolf Georg Beutel** [1] , **Oliver Niehuis** [2] , **Hans Pohl** [Corresp. 1]

[1] Institute of Zoology and Evolutionary Research, Friedrich Schiller University Jena, Jena, Thuringia, Germany

[2] Dept. of Evolutionary Biology and Ecology, Albert Ludwig University Freiburg, Freiburg, Germany

[3] Functional Morphology and Biomechanics, Zoological Institute, Christian-Albrechts-Universität zu Kiel, Kiel, Germany

[4] Institute for Photon Science and Synchrotron Radiation (IPS), Karlsruhe Institute of Technology (KIT), Karlsruhe, Germany

[5] Laboratory for Applications of Synchrotron Radiation (LAS), Karlsruhe Institute of Technology (KIT), Karlsruhe, Germany

Corresponding Authors: Kenny Jandausch, Hans Pohl
Email address: kenny.jandausch@uni-jena.de, hans.pohl@uni-jena.de

Traumatic insemination describes an unusual form of mating during which a male penetrates the body wall of its female partner to inject sperm. Females unable to prevent traumatic insemination have been predicted to develop either traits of tolerance or of resistance, both reducing the fitness costs associated with the male-inflicted injury. The evolution of tolerance traits has previously been suggested for the bed bug. Here we present data suggesting that tolerance traits also evolved in females of the twisted-wing parasite species *Stylops ovinae* and *Xenos vesparum.* Using micro-indentation experiments and confocal laser scanning microscopy, we found that females of both investigated species possess a uniform resilin-rich integument that is notably thicker at penetration sites than at control sites. As the thickened cuticle does not seem to hamper penetration by males, we hypothesise that thickening of the cuticle resulted in reduced penetration damage and loss of haemolymph and in improved wound sealing. To evaluate the evolutionary relevance of the *Stylops*-specific paragenital organ and penis shape variation in the context of inter- and intraspecific competition, we conducted attraction and interspecific mating experiments, as well as a geometric-morphometric analysis of *S. ovinae* and *X. vesparum* penises*.* We found that *S. ovinae* females indeed attract sympatrically distributed congeneric males. However, only conspecific males were able to mate. In contrast, we did not observe any heterospecific male attraction by *Xenos* females. We therefore hypothesise that the paragenital organ in the genus *Stylops* represents a prezygotic mating barrier that prevents heterospecific matings.

1 **Have female twisted-wing parasites (Insecta: Strepsiptera) evolved**
2 **tolerance traits as response to traumatic penetration?**

4 Kenny Jandausch[1,2*], Jan Michels[3], Alexander Kovalev[3], Stanislav N. Gorb[3], Thomas van de

5 Kamp[4,5], Rolf G. Beutel[1], Oliver Niehuis[2] and Hans Pohl[1*]

7 [1] Entomology Group, Institut für Zoologie und Evolutionsforschung, Friedrich-Schiller-

8 Universität Jena, Erbertstraße 1, 07743 Jena, Germany

9 [2] Dept. of Evolutionary Biology and Ecology, Albert Ludwig University Freiburg, Hauptstraße 1,

10 79104 Freiburg, Germany

11 [3] Functional Morphology and Biomechanics, Zoological Institute, Christian-Albrechts-

12 Universität zu Kiel, Am Botanischen Garten 1–9, 24118 Kiel, Germany

13 [4] Institute for Photon Science and Synchrotron Radiation (IPS), Karlsruhe Institute of

14 Technology (KIT), Hermann-von-Helmholtz-Platz 1, 76344, Eggenstein-Leopoldshafen,

15 Germany

16 [5] Laboratory for Applications of Synchrotron Radiation (LAS), Karlsruhe Institute of

17 Technology (KIT), Kaiserstraße 12, 76131, Karlsruhe, Germany

19 *Correspondence: kenny.jandausch@uni-jena.de (K.J.), hans.pohl@uni-jena.de (H.P.)

21 Submission admin: Hans Pohl, hans.pohl@uni-jena.de

23 Keywords: micro-indentation, confocal laser scanning microscopy, resilin, female tolerance

24 traits, interspecific competition

Abstract

Traumatic insemination describes an unusual form of mating during which a male penetrates the body wall of its female partner to inject sperm. Females unable to prevent traumatic insemination have been predicted to develop either traits of tolerance or of resistance, both reducing the fitness costs associated with the male-inflicted injury. The evolution of tolerance traits has previously been suggested for the bed bug. Here we present data suggesting that tolerance traits also evolved in females of the twisted-wing parasite species *Stylops ovinae* and *Xenos vesparum.* Using micro-indentation experiments and confocal laser scanning microscopy, we found that females of both investigated species possess a uniform resilin-rich integument that is notably thicker at penetration sites than at control sites. As the thickened cuticle does not seem to hamper penetration by males, we hypothesise that thickening of the cuticle resulted in reduced penetration damage and loss of haemolymph and in improved wound sealing. To evaluate the evolutionary relevance of the *Stylops*-specific paragenital organ and penis shape variation in the context of inter- and intraspecific competition, we conducted attraction and interspecific mating experiments, as well as a geometric-morphometric analysis of *S. ovinae* and *X. vesparum* penises. We found that *S. ovinae* females indeed attract sympatrically distributed congeneric males. However, only conspecific males were able to mate. In contrast, we did not observe any heterospecific male attraction by *Xenos* females. We therefore hypothesise that the paragenital organ in the genus *Stylops* represents a prezygotic mating barrier that prevents heterospecific matings.

Introduction

48 Sexual reproduction and copulation occur in many different varieties across the animal kingdom.

49 One of the most bizarre forms of sexual interaction is traumatic mating, which involves the

50 injury of one sexual partner during copulation. In one particular form of traumatic mating,

51 traumatic penetration (*Lange et al., 2013*), the female gets injured during the mating process, but

52 receives no sperm. In contrast, traumatic mating resulting in the injection of sperm and the

53 insemination of the female is referred to as traumatic insemination (*Lange et al., 2013*).

54 Traumatic insemination occurs in different groups of animals, such as flatworms, snails and

55 slugs, annelid worms, and arthropods (*Lange et al., 2013*; *Tatarnic, Cassis & Siva-Jothy, 2014*;

56 *Brand, Harmon & Schaerer, 2022*). However, one of the best known and studied organisms in

57 this context is the bed bug (*Cimex lectularius*) (*Michels, Gorb & Reinhardt, 2015*; *Reinhardt,*

58 *Anthes & Lange, 2015*; *Brand et al., 2022*), in which traumatic insemination occurs within a

59 paragenital organ: the spermalege.

60 Traumatic insemination leads to injuries of females and is recognised as an example of sexual

61 conflict (*Lange et al., 2013*; *Tatarnic et al., 2014*). Females unable to avoid unnecessary mating

62 are predicted to likely evolve resistance traits or tolerance traits that reduce the fitness costs

63 associated with sexual interaction with males. Resistance traits, which reduce the fitness of the

64 copulating male(s), can result in a co-evolutionary arms race. Such arms races are generally

65 thought to lead to accelerated trait exaggeration, such as the formation of species-specific

66 differences in copulatory organs (*Arnqvist & Rowe, 2002*; *Parker, 2006*; *Lange et al., 2013*).

67 *Michels et al. (2015)* found evidence for female tolerance traits (*i.e.*, traits that reduce the fitness

68 costs associated with a sexually conflicting interaction of the female without decreasing the

69 fitness of the male) in the form of resilin in the spermalege in bed bugs. The elastomeric protein

70 resilin seals the sexually imposed wounds and physically facilitates copulation by males (*Michels*

71 *et al., 2015*, p. 6).

72 The endoparasitic insect order Strepsiptera comprises ca. 600 described species. It is

73 characterised by numerous derived characters of all life stages and in both sexes (*Pohl & Beutel,*

74 *2008*). All species of the order display extreme sexual dimorphism. The males are free-living

75 (Fig. 1A, C); the only function of their extremely short life span of a few hours is to find females

76 and to mate. The females are usually obligatory endoparasites of other insects, in which they stay

77 during most of their larval development and as adults (Fig. 1B, D). Only females of the family

78 Mengenillidae are a notable exception, as they are free-living in the adult stage. Female

79 Strepsiptera are wingless and structurally strongly simplified, as compared to the males. Their

80 genital apparatus is extremely reduced: ovaries, vagina, receptacula seminis, genital chamber,

81 bursa copulatrix, and accessory glands are missing, and the eggs float freely in the hemolymph.

82 A single birth organ is present in females of Mengenillidae, with an opening in the region of

83 sternite VII through which the minute (ca. 200–250 µm) primary larvae are released.

84 The genera *Stylops* and *Xenos* investigated in the present study belong to the clade Stylopidia,

85 whose members utilise only pterygote insects as hosts and whose females are obligatory

86 endoparasites. Females of Stylopidia are characterised by secondary tagmosis: head, thorax, and

87 the anterior part of abdominal segment I form a compact cephalothorax, while antennae,

88 compound eyes, and legs are missing. The large sack-shaped posterior portion of the body

89 remains within the host's abdomen, whereas the cephalothorax is exposed. A secondary

90 copulation opening is located in the exposed cephalothorax. On the ventral side of the

91 cephalothorax, between head and prosternum, a birth opening is present in the majority of

92 species. This is the external opening of the brood canal, which is connected with the birth organs

93   in the abdomen. The birth opening enables the primary larvae to leave the females and is used in

94   most species for insemination (Stylopiformia). In Corioxenidae, insemination occurs either in the

95   region of the mouth opening or in the membranised pleural region (*Pohl & Beutel, 2008*). The

96   cuticle of the female is three-layered, as the female does not shed its larval exuviae. The cuticle

97   layers are detached in the ventral area and form the brood canal. The exuvia of the second larval

98   stage is strongly sclerotised in the cephalothoracic region, thinning only at the birth opening. The

99   exuvia of the tertiary larva is extremely thin and weakly sclerotised. (Fig. 2A, B).

100   The endoparasitic lifestyle of female Stylopidia has strongly influenced the mating strategy and

101   the mating behaviour of its species, as only the female's cephalothorax protrudes from the host's

102   abdomen (Fig. 1B, D). In *S. ovinae*, traumatic insemination takes place at a paragenital organ

103   (po) located in front of the birth opening (*Peinert et al., 2016*) (Fig. 2A, 3A), while in *X.*

104   *vesparum*, traumatic insemination occurs at the anterior part of the brood canal (bc) (Fig. 2B,

105   3B). However, *Beani et al. (2005)* discussed an alternative sperm route in *X. vesparum*, namely

106   by release of sperm into the brood canal: the sperm could then reach the hemocoel of the female

107   via the birth organs.

108   Previous studies have shown that the cuticle of the paragenital organ of *S. ovinae* and the cuticle

109   of the anterior brood canal of *X. vesparum* is about three times thicker than the cuticle in spatial

110   proximity (*Löwe, Beutel & Pohl, 2016*; *Peinert et al., 2016*; *Richter et al., 2017*). However, the

111   material composition of the cuticle at specific penetration sites has not been studied and

112   compared to that of the surrounding areas. This information could give additional clues whether

113   Strepsiptera have evolved resistance traits or tolerance traits in response to traumatic penetration.

114   The penises of different species of *Stylops* vary greatly in shape and size, whereas those of males

115   of *Xenos* differ almost exclusively in size (Fig. 4). Variation in penis shape, as reported for

116   *Stylops,* has so far only been described from the genus *Caenocholax* (Myrmecolacidae)

117   (*Kathirithamby et al., 2015*). The varying shape and size of the intromittent organs of different

118   *Stylops* species could be either the result of intersexual co-evolution or avoidance of

119   interbreeding between sympatric occurring congeners. Following *Eberhard (2004a)*, females

120   encountering males may be passively protected via species-specific pheromones, for example by

121   decreasing the chance of interspecific mating.

122   It is interesting to note that several of the 67 described *Stylops* species (*Straka, Jůzová & Nakase,*

123   *2015*) occur in sympatry and can be encountered in the same habitat at the same time of the year

124   (*e.g.*, at least three different *Stylops* species have been recorded flying in March in the vicinity of

125   Jena; HP, pers. obs.). In contrast, out of the 32 described *Xenos* species, only very few occur in

126   sympatry (*e.g.*, only two species in the Western Palearctic, one likely restricted to Libya, while

127   the other one is widespread). Furthermore, *Eberhard (2004b)* concluded that species-specific

128   traits in males are missing when females lack specific contact organs associated with copulation.

129   We hypothesise that the paragenital organ of *Stylops* is such a specific contact organ, which

130   suggests that the male genital armature will be more species-specific in this genus. To date it

131   remains unclear whether heterospecific copulations or heterospecific attraction of Strepsiptera

132   occurs in nature and if so, whether the species-specific morphology of the females' paragenital

133   organs pose a significant prezygotic reproductive barrier that prevents penetration by

134   heterospecific males.

135   We combined observational and experimental methods to address the question of whether

136   *Stylops* and *Xenos* females evolved resistance traits or tolerance traits as counter-adaptations

137   against traumatic wounding. We used confocal laser scanning microscopy to evaluate the

138   material composition of the cuticle at the wounding sites of *S. ovinae* (paragenital organ) and *X.*

139   *vesparum* (anterior brood canal) as well as at surrounding areas. We specifically assessed the

140   presence of resilin, a soft and elastic protein found in large proportions in the cuticle of the

141   spermalege of female bed bugs (*Michels et al., 2015*). We then measured the force required to

142   penetrate the cuticle of the paragenital organ of *S. ovinae* and the anterior brood canal of *X.*

143   *vesparum* using micro-indentation. We compared the results to the force necessary to penetrate

144   the cuticle in control areas.

145   To clarify the question why the penises of different *Stylops* species strongly differ in size and

146   shape, but not those of *Xenos*, we used field experiments to assess whether virgin females of both

147   species attract heterospecific males. We subsequently used laboratory mating experiments to test

148   whether heterospecific *Stylops* males are able to anchor and penetrate the female paragenital of

149   *S. ovinae* with their penis. Additionally, we reconstructed the three-dimensional morphology of

150   the penises and the female paragenital organ in *Stylops* using X-ray computed tomography to

151   assess the morphological fit of the two organs. Positive correlation of shape and size of penises

152   and paragenital organs of different *Stylops* species may indicate an interspecific copulatory

153   barrier comparable to a lock-and-key mechanisms. Finally, we used 3D models of penises of *S.*

154   *ovinae* and *X. vesparum* to estimate the extent of intraspecific variation using geometric

155   morphometrics. Comparing the magnitude of intraspecific penis variation of both investigated

156   species could indicate whether this contributed to the higher diversification of penis morphology

157   on the genus level.

158   **Material and Methods**

159   **Studied insects**

160   A total of 70 *Andrena vaga* (Hymenoptera, Andrenidae) parasitised by *S. ovinae* were collected

161   in Langerwehe (North Rhine-Westphalia, Germany) (February 16, 2020, and March 11, 2021, by

162   E. Holtappels, K. Jandausch, H. Pohl, and D. Tröger). During transport and preparation of the

163   experiments, the bees were kept dark in glass vessels (0.5 L) half filled with moist sand at ~4 °C

164   to prevent males of *S. ovinae* from hatching.

165   The hosts of *X. vesparum*, *Polistes dominula* (Hymenoptera, Vespidae), were collected in

166   Mettenheim (Rhineland-Palatinate, Germany) (July 1, 2018; July 21, 2020, and August 11, 2021,

167   by K. Jandausch, H. Pohl and D. Tröger) on a trumpet creeper bush (*Campsis radicans*).

168   Parasitised *P. dominula* are attracted to trumped creeper bushes and feed on extrafloral gland

169   secretions (*Beani et al., 2018*). Wasps collected in 2018 and 2021 were used for the attraction

170   experiments (see below). A total of 137 wasps were collected in 2020 for the micro-indentation

171   experiments. In the laboratory, each wasp was assigned to one of four groups: wasps with

172   extruded female *X. vesparum* (n = 32), wasps with extruded male puparia (n = 28), wasps with

173   extruded females and male puparia (n = 3), and wasps without externally visible infestation (n =

174   40). Only one male puparium was empty, indicating that the majority of females were

175   unfertilised. All parasitised wasps were kept in small groups (n = 5–8) in glass vessels (0.5 L)

176   covered with gauze at room temperature and were fed *ad libitum* with water and diluted honey.

177   Wasps without externally visible infestation were kept in an "aerarium" (40 cm x 40 cm x 60

178   cm) (Papa Papillon, Bern, Switzerland) and checked every day for freshly extruded *X. vesparum*.

179   One female specimen of *S. melittae* (ID: SFl87) and one of *S. hammella* (ID: SFc12) preserved in

180   ethanol were provided by Jakub Straka.

181   **Confocal laser scanning microscopy**

182   Cephalothoraces of a virgin female *S. ovinae* and of a virgin female *X. vesparum* were dissected,

183   transferred to glycerol (≥ 99.5 %, free of water, two times distilled; Carl Roth GmbH & Co. KG,

184   Karlsruhe, Germany) and mounted in glycerol on object slides with high-performance cover slips

185   (Carl Zeiss Microscopy GmbH, Jena, Germany) as described earlier (*Michels & Büntzow, 2010*;

186   *Michels & Gorb, 2012*). Four autofluorescences exhibited by the cephalothoracic cuticle

187   structures were visualised with a ZEISS LSM 700 confocal laser scanning microscope (Carl

188   Zeiss Microscopy GmbH), four solid-state lasers and bandpass and longpass emission filters as

189   previously described (*Michels & Gorb, 2012*; *Michels et al., 2015*). The microscope system was

190   controlled by the software ZEISS Efficient Navigation 2009 (ZEN 2009, Carl Zeiss Microscopy

191   GmbH). A ZEISS Plan-Apochromat lens with a numerical aperture of 0.45 (Carl Zeiss

192   Microscopy GmbH) was applied. Using ZEN 2009, a maximum intensity projection (MIP) was

193   created from each of the obtained data sets. The four different autofluorescence visualisation

194   results shown on the MIPs were colour-coded and overlaid as described earlier (*Michels & Gorb,*

195   *2012*). The resulting micrographs show differences in the autofluorescence composition of the

196   analysed cuticle structures and indicate differences in the material composition of these

197   structures. Red cuticle structures consist mainly of strongly sclerotised chitinous material, green

198   ones are chitinous and are weakly sclerotised or non-sclerotised and membranous, and blue ones

199   contain large proportions of resilin (*Michels & Gorb, 2012*).

200   **Specimen preparation**

201   Living females were extracted from their hosts with fine tweezers immediately before the micro-

202   indentation experiments. The strongly sclerotised outer cuticle of the cephalothorax was removed

203   to gain access to the penetration sites. The cephalothoraces were then fixed with micro-needles

204   on a silicon block (Silicone HR-N, Reckli, Herne, Germany). Two types of fixations were used

205   when handling *S. ovinae*: to make the ventral wall of the paragenital organ (wounding site)

206   accessible, the females were fixed with the morphological dorsal side directed upwards, and the

207   head area of the female was folded back. To expose the anterior part of the brood canal (control

208   site), females were fixed with the ventral side directed upwards. The brood canal was chosen as

209   the control site for *S. ovinae,* as it resembles the location where traumatic penetration takes place

210   in other families of Strepsiptera (*e.g.*, Xenidae). Females of *X. vesparum* were fixed exclusively

211   with the ventral side directed upwards, as wounding and control sites are located on the same

212   side. At the wounding sites, micro-indentation in *S. ovinae* and in *X. vesparum* was carried out in

213   the areas where mating signs are located in mated females (Fig. 3). In *X. vesparum*, reference

214   measurements at control sites were carried out at the posterior end of the brood canal where the

215   cuticle is much thinner, representing the general state of the cuticle at the cephalothorax. All

216   preparations were performed using a stereomicroscope (Olympus SZX12, Tokyo, Japan).

217   **Micro-indentation experiments**

218   Micro-indentation experiments were carried out on living virgin females without mating signs.

219   We studied 24 females of *S. ovinae* (wounding site: 14; control site: 10) and twelve females of *X.*

220   *vesparum*. In *X. vesparum*, we performed both measurements on the same females. The force to

221   penetrate the cuticle of the females was measured by inserting steel micro-needles with

222   diameters of 5.6 μm when studying *S. ovinae* and 4.1 μm when studying *X. vesparum*. In

223   comparison, the tips of the penises of *S. ovinae* measured on average 2.8 μm (n = 3, min. 2.6 μm,

224   max. 3.0 μm, and those of *X. vesparum* measured on average 0.8 μm (n = 3, min. 0.7 μm, max.

225   0.9 μm). All tips were analysed using scanning electron micrographs of the penises and tips of

226   the micro-needles. The needle was directly glued to a 10-g force transducer (World Precision

227   Instruments, USA) with cyano-acrylate glue (Ergo 5925 Elastomer, Kisling AG, Wetzikon,

228   Switzerland). The force transducer was attached to a motorised micro-manipulator. To perform

229   the indentation experiments, the force transducer was moved down with 200 μm/s velocity.

230   During the experiments, the females were moistened with a drop of tap water to prevent drying

231   artefacts. Each specimen was penetrated several times on slightly different positions. The whole

232   system was connected to a computer running the software AcqKnowledge 3.7.3 (Biopac System

233   Inc., Goleta, USA) (Fig. S2). This software was used to record and process the measured force

234   and time/travelled distance. All measurements were controlled visually with a stereomicroscope

235   (LEICA MZ 12.5, Wetzlar, Germany) to guarantee the penetration on the chosen location.

236   Individual measurements were documented using a video camera (Basler piA1900-32g, Basler

237   Vision Technologies) attached to the stereomicroscope. The software SteamPix5 (Norpix Inc.,

238   Montreal, Canada) was used to record the videos.

239   **Scanning electron microscopy**

240   Scanning electron micrographs of the penises of *S. ovinae* and of *X. vesparum* were taken with a

241   Philips ESEM XL30 (Philips, Amsterdam, Netherlands) (Fig. S3). The same equipment was used

242   to obtain micrographs of the tips of the steel microneedles used in the micro-indentation

243   experiments. The penises were air-dried, glued to a microneedle, fixed on a rotatable specimen

244   holder (*Pohl, 2010*), and sputter-coated with gold using an Emitech K500 (sample preparation

245   division, Quorum Technologies Ltd., Ashford, England).

246   **Attraction experiments**

247   In 2020, four bees, and in 2021, eight bees from Langerwehe parasitised with *S. ovinae* females

248   were kept in an "aerarium" (see above). The "aerarium" was placed in the field and orientated in

249   the direction of the wind flow to increase the dispersion of female pheromones. The attraction

250   experiments were conducted on March 18 and 19, 2020, and between March 24 and March 26

251   and on March 29, 2021, in the vicinity of Jena (Thuringia, Germany). Approaching males were

252   collected from the gauze of the "aerarium" with an aspirator. In 2020, two, and in 2021, 40 of the

253   attracted males were taken to the lab alive in snap-cap vials. To keep the males vital for the

254   mating experiments, they were transported in a cold bag at ~5 °C. The remaining males were

255   immediately fixed in 100% ethanol.

256   An identical setup was used to attract male *X. vesparum* in the backyard of the Phyletisches

257   Museum Jena (Thuringia, Germany). On July 18, 2018, five, and on August 16, 2021, eight

258   infected wasps from Mettenheim were placed in an "aerarium". *Beani et al. (2018)* carried out

259   similar attraction experiments with parasitised wasps in small vials to attract males of *X.*

260   *vesparum*. In contrast to *S. ovinae*, males of *X. vesparum* were fixed in 70% ethanol after

261   collecting them from the gauze, as no further mating experiments were carried out with this

262   species.

263   **Species identification of the attracted males**

264   To identify *Stylops* species, we analysed a 605-bp-long fragment of the mitochondrial gene COI

265   in all males collected in 2020 and in the four males that we used in the mating experiment in

266   2021. The DNA was extracted from legs using the QIAGEN QIAamp DNA Micro, following the

267   protocol of the manufacturer. PCR amplification was carried out with the oligonucleotide

268   primers 5'-TCW ACA AAT CAT AAA ATA ATT GG-3' (CO122For), 5'-TCC TCC TCC TAA

269   AGG RTC RAA-3' (CO16669Rev), 5'-TWT CWA CHA AYC ATA ARG ATA TTG G-3'

270   (Cox1LCO_DEG) and 5'-TCA ATT TCC AAA YCC YCC YAT-3' (Cox1ALEX_DEG)

271   published by *Folmer et al. (1994)*, *McMahon, Hayward & Kathirithamby (2009)*, and *Jůzová,*

272   *Nakase & Straka (2015)*. PCRs were performed with the Invitrogen Taq DNA Polymerase for

273   standard PCR (Thermo Fisher Scientific Inc., Waltham, USA) including dNTPs, PCR buffer,

274   MgCl$_2$, and *Taq* Polymerase. Applied primers were manufactured by Metabion GmbH (Munich,

275   Germany). PCRs started with a 180 s initial phase at 94 °C, followed by 30 cycles of 45 s at

276   94 °C, 30 s at 50 °C and 90 s. at 72 °C, and ended with one final extension at 72 °C for 10 min.

277   Products were purified using ExoProStar 1-Step (Global Life Sciences Solutions USA LLC,

278   Marlborough, USA). For direct bidirectional Sanger sequencing, samples were sent to Macrogen

279   (Amsterdam, Netherlands). After removing the primer binding sites, forward and reverse

280   sequences of each specimen were aligned using Geneious prime 2021.0.3 and compared to

281   reference sequences for the genus *Stylops* established by *Jůzová et al. (2015)* (Fig. S4). All other

282   males were determined by comparing their penis to the penises of the barcoded males.

283   The attracted *Xenos* males were identified with the key provided by *Kinzelbach (1978)*.

284   **Mating experiments**

285   In order to determine whether the attracted males are able to insert their penis into the paragenital

286   organ and anchor themselves within virgin females of *S. ovinae*, we followed the method

287   established by *Peinert et al. (2016)*. The mating experiments were carried out directly after

288   collecting the specimens in the field and returning with them to the lab to ensure the vitality of

289   the short-lived males. The copulations were initiated in transparent plastic trays (4 cm diameter,

290   1 cm high) at 21 ± 1 °C. The metasoma of each parasitised host was removed and was attached

291   directly to modelling clay with its anterior end on the bottom of the trays. The males were placed

292   one at a time in plastic dishes, and the dishes' opening was closed with a transparent lid to

293   prevent the males from escaping. After about 2 minutes, when each male had mounted the

294   metasoma of the host bee and attempted to mate with the female, the males were removed and

295   fixed in 100 % ethanol for later species identification unless otherwise stated. Note that we

296   determined all males after the experiments, either by barcoding or by comparing the penises of

297   the males with those of barcoded males. Mating attempts were recorded with a Canon EOS 7D

298   digital SLR equipped with a Canon MP-E 65 mm macro lens (Canon, Krefeld, Germany) or an

299   Apple iPhone SE (second generation) (Cupertino, California, U.S.) through the eyepiece of a

300   Leica MS 5 stereomicroscope (Leica, Wetzlar, Germany). We used a cold light source (KL 750,

301   Schott, Mainz, Germany) as lighting.

302   In total, we introduced 18 of the attracted males to females of *S. ovinae* and tested whether they

303   tried to mate or not. The following mating experiments were performed with virgin females of *S.*

304   *ovinae* as described in the preceding paragraph: one male of *S. hammella* with two females

305   (video recording), and one male of *S. ovinae* with two females. This latter male mated with one

306   of the females and was fixed in copula with 100 % ethanol cooled to -80 °C for a µCT scan.

307   Eleven males of *S. melittae* were successively placed to one female (video recording). To detect

308   possible injury to females by these heterospecific males during their mating attempts, four males

309   of *S. melittae* were each placed to four infested host metasomas. Of these, two host metasomas

310   were parasitised by one, one by two, and one by three virgin females. Since the penetration site is

311   marked by a melanised spot on the cuticle one day after mating, we stored these females in their

312   host metasoma for 48 h after the mating attempts in the refrigerator at 5 °C. To document the

313   mating signs, we extracted the females from the host, removed the outer cuticle of the

314   cephalothorax, dehydrated the specimens in an ascending ethanol series, and mounted the

315   cephalothorax in Euparal (Carl Roth, Karlsruhe, Germany) on microscope slides. Photographs

316   were taken with a Canon EOS 7D digital SLR equipped with a Mitutoyo M Plan Apo 10x lens

317   (Mitutoyo, Kawasaki, Japan). The slides were illuminated with two flashlights (Yongnuo

318   Photographic Equipment, Shenzhen, China).

319   **X-ray computed tomography and 3D-reconstruction**

320 One female and one male of *S. hammella*, one male of *S. melittae*, and one pair of *S. ovinae* fixed

321 in copula (see mating experiments) were scanned in pure ethanol at the Imaging Cluster at the

322 KIT Synchrotron Radiation Facility using a polychromatic X-ray beam produced by a 1.5 T

323 bending magnet spectrally filtered by 0.5 mm Al. A fast indirect detector system was employed,

324 consisting of a 13 μm LSO:Tb scintillator (*Cecilia et al., 2011*), a diffraction limited optical

325 microscope (Optique Peter) (*Douissard et al., 2012*), and a 12-bit pco.dimax high speed camera

326 with 2,016 x 2,016 pixels. Scans were done by taking 3,000 projections at 70 fps over an angular

327 range of 180°. An optical magnification of 10x resulted in an effective pixel size of 1.22 μm. The

328 control system concert (*Vogelgesang et al., 2016*) was employed for automated data acquisition

329 and online reconstruction of tomographic slices for data quality assurance. Data processing

330 included flat field correction and phase retrieval of the projections based on the transport of

331 intensity equation (*Paganin et al., 2002*). X-ray beam parameters for algorithms in the data

332 processing pipeline were computed by *syris (Faragó et al., 2017)*. The execution of the

333 pipelines, including tomographic reconstruction, was performed by the UFO framework

334 (*Vogelgesang et al., 2012*). One female of *S. melittae* was scanned in a SkyScan221 micro-CT

335 (FSU Jena) with beam strength of 40 kV and 300 μA. In a 360° scan, pictures were taken every

336 0.2° with an exposure time of 5,800 ms. A pixel size of 1.22 μm was achieved. We segmented

337 tomographic data using Dragonfly 4.1 for Windows (Object Research Systems [ORS] Inc,

338 Montreal, Canada, 2019) and used VGStudiomax 2.0.5 (Volume Graphics, Heidelberg,

339 Germany) for visualization and rendering.

340 **Geometric morphometrics**

341 To estimate the intraspecific variation, penises of 18 specimens of *S. ovinae* (Niedringhaussee,

342 Lower Saxony, Germany) and of 17 specimens of *X. vesparum* (Jena, Thuringia, Germany) were

343 carefully removed with fine tweezers and dried at the critical point with a Emitech K850 Critical

344 Point Dryer (Sample preparation division, Quorum Technologies Ltd., Ashford, England).

345 Penises were transferred into a plastic pipette tip and scanned in a SkyScan221 micro-CT (FSU

346 Jena) with beam strength of 40 kV and 200 µA. In a 360° scan, pictures were taken every 0.2°

347 with an exposure time of 2,300 ms. A pixel size of 0.7 µm was achieved. Segmentation was

348 performed with Dragonfly 4.1 for Windows (Object Research Systems Inc, Montreal, Canada,

349 2019). Exported *stl* files were smoothed and the polygons were reduced and rendered with

350 Blender before exportation as *obj* files (Blender Foundation, Amsterdam, Netherlands).

351 Landmarks and semilandmarks were placed with Stratovan Checkpoint (Stratovan Cooperation,

352 Davis, USA).

353 **Landmarks**

354 Nine landmarks and 126 semilandmarks on two curves were placed on the 3D objects to describe

355 the overall size and outline shape of the penises. Landmark 1 describes the proximal edge of the

356 phallotreme. Landmark 2 was placed at the deepest point of the ventral angle of the acumen (Fig.

357 S3). Landmark 3 represents the transition from the flat distal part of the penis to the broader

358 base, and landmark 4 marks the posterior edge of the sclerotised penis base. Along these first

359 four landmarks, 54 semilandmarks where projected to represent the posterior outline of the penis

360 shape in detail. Landmark 5 was placed at the distal edge of the phallotreme, followed by

361 landmark 6 at the tip of the acumen. Landmark 7 marks the maximum point of the dorsal

362 curvature of the entire acumen. Landmark 8 represents the dorsal spine. Landmark 9 represents

363 the anterior edge of the sclerotised penis base. A curve consisting of 72 semilandmarks was

364 placed between landmark 5 to landmark 9 to describe the shape of the acumen and the anterior

365 outline.

366 **Statistical analysis**

367 We conducted a total of 146 penetration force experiments (*S. ovinae* wounding site: 43; *S.*

368 *ovinae* control site: 41; *X. vesparum* wounding site: 38; *X. vesparum* control site: 36). We

369 analysed 30 measurements from the wounding site of *S. ovinae,* 40 measurements from the

370 control site of *S. ovinae*, 38 measurements from the wounding site of *X. vesparum*, and 36

371 measurements from the control site of *X. vesparum*.

372 For statistical analysis and significance tests, we used the software RStudio (R Core Team,

373 Auckland, New Zealand). Boxplots and raw diagrams were drawn with the same software. We

374 applied the Shapiro-Wilk test for testing for normal distribution and F test for testing for equality

375 of variances among independent datasets. The level of significance was checked with a Kruskal-

376 Wallis test and with a Wilcoxon pairwise comparison (including Bonferroni-Holm correction). In

377 case of the data of *X. vesparum*, we used Levene's test for assessing the equality of variances

378 instead of applying an F test, because the data did not follow a normal distribution (Shapiro-Wilk

379 test: $p = 0.03403307$ [wounding site] and $p = 0.01891762$ [control site]). The data of *S. ovinae*,

380 however, were normally distributed (Shapiro-Wilk test: $p = 0.09288335$ [wounding site] versus p

381 $= 0.7888944$ [control site]) (Table 1).

382 Geometric morphometric analysis was carried out with RStudio (R Core Team, Auckland, New

383 Zealand) and the geomorph package (*Adams et al., 2021*; *Baken et al., 2021*). General Procrustes

384 analysis was performed using the gpagen function with semilandmarks allowed to slide between

385 landmarks by minimizing bending energy (define.sliders). Resulting centroid size for each

386 specimen was used for calculation of the coefficient of variance. PCA of the Procrustes shape

387 variables was performed with the function gm.prcomp and the results were visualized with the

388 packages pca3D and rgl to explore major aspects of the geometric variation.

389   **Image processing**

390   All images were processed with Adobe Photoshop Version 21.2.1 (Adobe Systems Incorporated,

391   San Jose, CA, USA). We used Adobe Illustrator Version 24.2.1 (Adobe Systems Incorporated,

392   San Jose, CA, USA) for labelling the plates and for drawings and processing diagrams.

393   **Results**

394   **Confocal laser scanning microscopy**

395   Major parts of the cephalothoracic cuticle of both investigated species contain large proportions

396   of resilin, including the areas where traumatic insemination takes place (Fig. 5). The composition

397   of the cuticle in the control areas does not differ from sites where traumatic insemination takes

398   place. In *S. ovinae*, the spiracles and the main tracheal stems of the cephalothorax consist of

399   sclerotised chitinous material (Fig. 5A). In contrast, different areas on the ventral side of the

400   cephalothorax are not or only weakly sclerotised. These include individual structures of the

401   cephalic area, patches of the lateral pro-, meso-, and metathoracic regions, as well as microtrichia

402   on the surface of abdominal segment I (Fig. 5A). The microtrichia covering almost the entire

403   ventral cephalothoracic surface of *X. vesparum* are apparently slightly more sclerotised than

404   those on the cephalothorax of *S. ovinae* (Fig. 5B). However, the spiracles, the main tracheal

405   stems, and the lateral regions of the cephalothorax of *X. vesparum* are less sclerotised than

406   corresponding areas in *S. ovinae*.

407   **Micro-indentation experiments**

408   The force required to penetrate the paragenital organ of *S. ovinae* (wounding site; see Fig. 5A)

409   with a micro-needle was statistically significantly higher (mean: 9.732 mN) than the force

410   required at a control site at the brood canal (see Fig. 5A) (mean: 4.578 mN) (Wilcoxon pairwise

411   comparison; p = 2.1e-08*; Table 1 and 2). Likewise, the force required to penetrate the anterior

412   brood canal (wounding site; see Fig. 5B) of *X. vesparum* was significantly higher (mean: 3.669

413   mN) than the force required at the posterior control site in the brood canal (see Fig. 5B) (mean:

414   2.003 mN) (Wilcoxon pairwise comparison ; p = 1.5e-08*; Table 1 and 2). The absolute forces

415   required to penetrate the cuticle were consistently higher in *S. ovinae* than in *X. vesparum*.

416   Critical stress (force per unit area) was calculated to compare the mechanical impact of the

417   intromittent devices on female structures in both species, independent of differences in the

418   diameter of the device. The highest mean value (0.402 GPa) was measured at the wounding sites

419   of *S. ovinae* (Fig. 6, Table 1). The mean critical stress at the corresponding control sites (0.186

420   GPa) proved to be statistically significantly lower (Wilcoxon pairwise comparison; p = 7.5e-09*)

421   (Tables 1 and 2). The critical stress value was significantly higher than critical stress values

422   obtained for measurements at wounding and at control sites of *X. vesparum* (Fig. 6, Tables 1 and

423   2). The critical stress at the wounding site of *X. vesparum* (mean value of 0.273 GPa) was

424   significantly higher than that at the control site (mean value of 0.149 GPa) (Wilcoxon pairwise

425   comparison; p = 2.7e-08*) (Tables 1 and 2).

426   **Attraction experiments**

427   During two consecutive days in 2020, we were able to attract a total of 18 *Stylops* males in the

428   field by exposing four *Andrena vaga* parasitised with females of *S. ovinae*. Using DNA

429   barcoding and/or morphology (i.e., the species-diagnostic shape of the penis), we identified the

430   18 captured *Stylops* males as *S. hammella* (two individuals), *S. melittae* (13 individuals) and *S.*

431   *ovinae* (three individuals). During four consecutive days in 2021, we attracted an additional 94

432   *Stylops* males by exposing eight *A. vaga* parasitised with females of *S. ovinae*. Of these, 91 were

433   identified as *S. melittae* and one as *S. ovinae*. Two specimens were accidentally crushed during

434 capture and remained unidentified. In 2018, we were able to collect 104 males of *X. vesparum*

435 during a single day, attracted by a single *P. dominula* female parasitised by a single *X. vesparum*

436 female. In 2021, we additionally collected 81 males of *X. vesparum* by exposing ten *P. dominula*,

437 each parasitised by *X. vesparum* females during a single day. Note that each of the above females

438 of *S. ovinae* and *X. vesparum* attracted multiple males simultaneously.

439 **Mating experiments**

440 All *Stylops* males of the attraction experiments, irrespective of their species identity, mounted the

441 parasitised host bee and searched for a suitable position on the bee's metasoma to mate with the

442 *S. ovinae* females. The male of *S. hammella* was unable to insert its penis into the paragenital of

443 two female *S. ovinae* and to anchor itself (Video S1). All *S. melittae* males were able to insert

444 their penises into the paragenital organ, but they were unable to anchor (Video S1). In three out

445 of six copulation attempts of *S. melittae* males with *S. ovinae* females, the female's cuticle was

446 punctured. However, none of the resulting scars in the cuticle were found at the terminal end of

447 the paragenital organs, the only location penetrated by conspecific males (pers. obs. HP and KJ),

448 but rather in the anterior region of the paragenital organ (Fig. S1). Only the conspecific male was

449 able to perforate the terminal part of the female's paragenital organ (fixed in copula, µCT scan).

450 **Co-adaptation of the penises with the females' paragenital organs**

451 We used µCT scans of the penises and of the paragenital organs of *S. ovinae* (raw data taken

452 from *Peinert et al. (2016)*), *S. hammella,* and *S. melittae*, and digitally inserted the penises into

453 the paragenital organs with VGStudiomax 2.0.5 (Volume Graphics, Heidelberg, Germany).

454 Doing so illustrated that the size and shape of a specific penis fits only with the paragenital organ

455 of conspecific females (Fig. 7).

Geometric morphometrics

456

457 By performing Generalised Procrustes analysis of the morphometric data of *S. ovinae* penises,

458 we calculated a mean centroid size of 1829.35, with a standard deviation of 84.88. The

459 coefficient of variation of 4.64% describes the extent of variation of *S. ovinae* penises with

460 respect to centroid size. Based on a 95% coincidence interval, one outlier was found among the

461 *S. ovinae* data.

462 The first three axes of the principal components analysis ordination plot explain 64.1% of the

463 sample shape variation of *S. ovinae* penises (Fig. 8C). PC1 explains 32.1% of the shape

464 variation. From negative to positive PCA values, the dorsal spine shifts towards the base of the

465 penis, resulting in a slightly s-shaped or in a non-s-shaped back of the acumen's dorsal outline

466 compared to penises related to lower values. Furthermore, the posterior bulge is shifted ventrad

467 towards higher values. PC2 accounts for 20.4% of the sample shape variation. Moving from

468 negative to positive PCA values, shape changes are expressed by a slightly shorter acumen and a

469 sharper ventral angle of the dorsal spine. PC3 describes 11.6% of the total sample shape

470 variation of *S. ovinae* and relates to a more prominent posterior bulge and slightly elongated

471 posterior spine for positive values.

472 Generalised Procrustes analysis of morphometric data of *X. vesparum* penises resulted in a mean

473 centroid size of 1243.18 with a standard deviation of 45.08. Regarding centroid size, the

474 variation is described by coefficient of variation of 3.6%. As in *S. ovinae*, an outlier was

475 identified among the data of *X. vesparum* based on a 95% confidence interval.

476 The first three principal components of the PCA explain 64.9% percent of the overall sample

477 shape variation. With a proportion of 38.7% of sample shape variation, negative PC1 values

478 associated with penises having a strongly curved posterior edge straightened towards positive

479   values. The shape variation also influences the dorsal curvature of the acumen, being less curved

480   with positive values than with negative ones. PC2 accounts for 14.1% of total sample shape

481   variation. Positive values are related to a slightly more downward tilted tip of the acumen for

482   positive PCA values as for negative values. PC3 describes 12.1% of the sample shape variation.

483   Going from negative to positive, the dorsal spine shifts more dorsad. This appearance leads also

484   to a more strongly bent dorsal curvature of the acumen in *X. vesparum*.

485   **Discussion**

486   Increased thickness and sclerotization of the insect cuticle are common adaptations to reduce the

487   risk of sexual wounding (*Merritt, 1989*; *Baer & Boomsma, 2006*; *Kamimura, 2007*; *Rönn,*

488   *Katvala & Arnqvist, 2007*; *Lange et al., 2013*; *Dougherty & Simmons, 2017*; *Matsumura et al.,*

489   *2017*). In *S. ovinae* and *X. vesparum*, the cuticle of females is weakly sclerotised and uniformly

490   rich in resilin. Most notably, however, it is also three times thicker at the wounding site than at

491   control sites in close spatial proximity. Note that the endoparasitic females are enclosed by the

492   exuviae of the secondary and tertiary larval stage, and that the former is strongly sclerotised,

493   thinning only at the birth opening. The males can only insert their penis at the strongly thinned

494   exuvia of the birth opening. The remaining exuvia of the secondary larva is not suitable for male

495   penetration. *Michels et al. (2015)* considered bed bugs as an example of a species in which the

496   females have evolved tolerance against traumatic mating. This is due to higher proportions of

497   resilin in the females' spermalege compared to surrounding areas of the abdomen. The flexibility

498   and resilience of resilin allow efficient sealing of the cuticle after penetration and help reducing

499   loss of haemolymph (*Michels et al., 2015*). At the same time, the forces required to pierce the

500   cuticle of the spermalege are notably lower than those at control sites. The high proportion of

501   resilin in the cuticle of the spermalege has been consequently interpreted as a response to

502   traumatic mating, as it facilitates piercing by the male genitalia. The increased thickness of the

503   integument in Strepsiptera requires a higher force to pierce the cuticle at the penetration sites

504   (compared to control sites). This result could indicate that Strepsiptera have evolved resistance

505   rather than tolerance against traumatic insemination. However, *Peinert et al. (2016)* found *S.*

506   *ovinae* males to be consistently able to penetrate their female partners within seconds, indicating

507   that the specific structure of the female cuticle does not seem to hamper penetration by males.

508   We consequently favour an alternative interpretation, namely that the thickened cuticle is also a

509   tolerance trait. As the weakly sclerotised integument of female strepsipterans is already rich in

510   resilin, further increasing the amount of this protein in the integument may not help to mitigate

511   the male-inflicted trauma on the female's integument. However, increased thickness of the body

512   wall could have such an effect. Potential positive effects of a thickened cuticle could be a

513   reduced risk of integument rupture, improved sealing of the copulation wounds, and reduction of

514   haemolymph loss.

515   We demonstrated that the sex pheromone emitted by *S. ovinae* females attracts not only

516   conspecific males, but also males of two additional congeneric species. In contrast, females of *X.*

517   *vesparum* attracted only conspecific males. The sympatric occurrence of congeneric species is

518   much more common in *Stylops* than in *Xenos*, whose species do not possess a paragenital organ

519   (*Kinzelbach, 1971*). In the Western Palearctic, only two species of *Xenos* are described (*X.*

520   *vesparum* and *Xenos zavattarii* (Pierce, 1911) (*Benda et al., 2022*), the latter only documented

521   from Tripoli, Libya). In contrast, 32 different species of *Stylops* are currently documented and

522   are accepted as valid species in the Western Palaearctic, and many of them occur in sympatry

523   (*Straka et al., 2015*). Male *Stylops* are known to hatch in synchronised masses during a few days

524   in late winter/early spring (*Grabert, 1953*; *Lauterbach, 1954*; *Tolasch, Kehl & Dötterl, 2012*;

525   *Lagoutte et al., 2013*). This situation most likely leads to copulation of one female with multiple

526   males and to increased interspecific competition. In contrast to males of *Stylops*, hatching of

527   males of *Xenos* is not synchronised. They are released over a period from mid-July until mid-

528   August (*Hughes et al., 2004*). Competition between males should consequently be comparatively

529   low. However, our attraction experiments showed that the elongated flight period of *X. vesparum*

530   does not mean that males of this species necessarily encounter females in lower frequency than

531   in *S. ovinae*. In both species, we found multiple males having been attracted by females in short

532   periods of time, even simultaneously. *Hughes et al. (2004)* and *Beani et al. (2018)* also observed

533   that several males of *X. vesparum* were attracted to *X. vesparum* females at the same time. We

534   consequently hypothesise that in *S. ovinae*, interspecific competition and intraspecific

535   competition for females are relatively high, whereas in *X. vesparum,* intraspecific competition is

536   prevalent across most of the distribution range.

537   *Kathirithamby et al. (2015)* speculated that females of Strepsiptera produce species-specific

538   pheromones to entice conspecific and to exclude heterospecific males. The sex pheromones are

539   produced by the Nassonow's glands which open on the ventral surface of the brood canal in the

540   female's cephalothorax (*Dallai et al. 2004*). As we found that the female sex pheromone of *S.*

541   *ovinae* attracts heterospecific males, another mechanism is (or additional mechanisms are) likely

542   in place to reduce the chance of heterospecific mating. In his review on the rapid divergent

543   evolution of sexual morphology, *Eberhard (2004b)* stated that species-specific traits in males are

544   typically present when specific contact organs exist in females. Males among different *Stylops*

545   species differ strongly in the shape and the size of their intromittent organ (*Kinzelbach, 1971*;

546   *Kinzelbach, 1978*) (Fig. 4A–E). The size of their penises positively correlates with the size of the

547   conspecific female paragenital organ, at least in all three investigated species. In contrast, the

548   penises in *Xenos* species differ only slightly in size and shape (*Kinzelbach, 1971*; *Kifune &*

549   *Maeta, 1975*; *Kifune & Maeta, 1985*; *Kifune, 1986*; *Kathirithamby & Hughes, 2006*; *Nakase &*

550   *Kato, 2013*; *Cook et al., 2020*) (Fig. 4F–I). We therefore hypothesise that the paragenital organ in

551   *Stylops* evolved as a species-specific contact organ for copulation. The proximal part and the

552   acumen (Fig. S3) of the penises vary in width and length among species (Fig. 4). Our mating

553   experiments on *S. ovinae* showed that only conspecific males are able to mate successfully.

554   Therefore, we conclude that interspecific mating is prevented by structural differences of the

555   paragenital organ of *Stylops* females. Hence the paragenital organ, in combination with the penis

556   shape, likely functions as a prezygotic barrier between different species. This barrier is

557   apparently missing in the genus *Xenos*, possibly because heterospecific mating does not occur or

558   is rare for other reasons.

559   It remains to be investigated whether intraspecific sexual conflict may further accelerate the

560   evolution of the genital morphology within the two sexes of *Stylops*. Intersexual conflict should

561   increase variation within a population. Therefore, we initially hypothesised that the variation of

562   the penis morphology is larger in *S. ovinae* than in *X. vesparum*. However, we found no

563   difference in the magnitude of interspecific variation between the two species, and the males'

564   intromittent organs of *S. ovinae* and *X. vesparum* vary to a similar extent (approximately 4% in

565   centroid size). Therefore, our results do not support this interpretation. However, they do not rule

566   out intraspecific sexual conflict either, as our assumption of intraspecific sexual conflict

567   restricted to species of *Stylops* could have been wrong.

568   **Conclusions**

569   The results of our study suggest that female strepsipterans of the genera *Stylops* and *Xenos* have

570   likely evolved tolerance traits against traumatic insemination. This is achieved by thickening of

571 the uniformly resilin-rich integument at the site of penetration. In contrast, female bed bugs

572 achieved tolerance by incorporating the elastomeric protein resilin at the site of penetration only.

573 This thickening in *Stylops* and *Xenos* does not seem to have any negative effect on the male

574 partner, who appears to be always able to pierce the penetration site within seconds. Whether or

575 not mating behaviour and morphological diversity of male penises and female paragenital organs

576 are directly correlated to mating success of either sex is the subject of future research. However,

577 we predict that tolerance traits in the context of traumatic insemination are more widespread in

578 insects than currently assumed.

579 **Acknowledgements**

580 We thank Eberhardt Holtappels (Langerwehe) for his help with collecting stylopised bees and

581 Irmgard and Hans Muth (Mettenheim) for the permission to collect wasps on their private

582 property. We also thank Daniel Tröger (Jena) for collecting infested bees and wasps.

583 Furthermore, we thank Jakub Straka (Praha) for providing material for this study, Adrian Richter

584 (Jena) for performing µCT scans, Alexander Stoessel for providing access to the equipment at

585 the Max-Planck-Institut für Menschheitsgeschichte (Jena), and Marcus Zuber and Tomás Farago

586 (both KIT) for their help at the beamline and with the reconstruction of synchrotron µCT data.

587 We acknowledge the KIT light source for provision of instruments at their beamlines. We also

588 thank the Institute for Beam Physics and Technology (IBPT) for the operation of the storage

589 ring, the Karlsruhe Research Accelerator (KARA). Furthermore, our thanks go to Brendon

590 Boudinot for helpful input to the manuscript. ON, HP, SG and RGB acknowledge the German

591 Research Foundation (DFG) for supporting this study (NI 1387/9-1; PO 1207/4-1; GO 995/46-1;

592 BE 1789/15-1). Finally, we thank Joseph Gillespie, Laura Beani, and Leon Lounibos for their

593 helpful suggestions, which helped improving the manuscript.

Author Contributions

594

595 H.P., O.N., R.G.B, and S.G. conceived the project and designed the experiments. Micro

596 indentation experiments were carried out by A.K., H.P, and K.J. CLSM visualizations and the

597 sample preparation required for them was performed by J.M. K.J. carried out the statistical

598 analysis. Barcoding and identification were performed by K.J. Attraction and mating

599 experiments were performed by H.P. and K.J. T.v.d.K. performed X-ray computed tomography.

600 Segmentation, 3D-modeling of the μCT-Data, and geometric morphometrics analysis was

601 executed by K.J. H.P. and K.J. prepared the figure plates and wrote the manuscript with helpful

602 input from all other authors.

Competing Interest

603

604 The authors declare no competing interests.

605

606 **Data Availability**

607 The following information was supplied regarding data availability:

608 MicroCT Data are available at Morphosource:

609 https://www.morphosource.org/projects/000430676.

610 - Copulating pair of *Stylops ovinae* CT Image Series; Media 000431013; MorphoSource DOI:

611 10.17602/M2/M431013

612 - Female cephalothorax of *Stylops hammmella* CT Image Series; Media 000430994;

613 MorphoSource DOI: 10.17602/M2/M430994

614 - Female cephalothorax of *Stylops melittae* CT Image Series; Media 000431002; MorphoSource

615 DOI: 10.17602/M2/M431002

616 - Penis of *Stylops hammmella* CT Image Series; Media 000430950; MorphoSource DOI:

617 10.17602/M2/M430950

618 - Penis of *Stylops melittae* CT Image Series; Media 000430981; MorphoSource DOI:

619 10.17602/M2/M430981

620 - 18 Penises of *Stylops ovinae* surface models

621   pmj:Strep_42/01: Media 000432425; MorphoSource DOI: 10.17602/M2/M432425

622   pmj:Strep_42/02: Media 000432431; MorphoSource DOI: 10.17602/M2/M432431

623   pmj:Strep_42/03: Media 000432437; MorphoSource DOI: 10.17602/M2/M432437

624   pmj:Strep_42/04: Media 000432442; MorphoSource DOI: 10.17602/M2/M432442

625   pmj:Strep_42/05: Media 000432448; MorphoSource DOI: 10.17602/M2/M432448

626   pmj:Strep_42/06: Media 000432454; MorphoSource DOI: [10.17602/M2/M432454](#)

627   pmj:Strep_42/08: Media 000432460; MorphoSource DOI: [10.17602/M2/M432460](#)

628   pmj:Strep_42/09: Media 000432466; MorphoSource DOI: [10.17602/M2/M432466](#)

629   pmj:Strep_42/10: Media 000432472; MorphoSource DOI: [10.17602/M2/M432472](#)

630   pmj:Strep_42/11: Media 000432478; MorphoSource DOI: [10.17602/M2/M432478](#)

631   pmj:Strep_42/12: Media 000432484; MorphoSource DOI: [10.17602/M2/M432484](#)

632   pmj:Strep_42/13: Media 000432489; MorphoSource DOI: [10.17602/M2/M432489](#)

633   pmj:Strep_42/14: Media 000432495; MorphoSource DOI: [10.17602/M2/M432495](#)

634   pmj:Strep_42/15: Media 000432501; MorphoSource DOI: [10.17602/M2/M432501](#)

635   pmj:Strep_42/16: Media 000432507; MorphoSource DOI: [10.17602/M2/M432507](#)

636   pmj:Strep_42/17: Media 000432512; MorphoSource DOI: [10.17602/M2/M432512](#)

637   pmj:Strep_42/19: Media 000432518; MorphoSource DOI: [10.17602/M2/M432518](#)

638   pmj:Strep_42/22: Media 000432529; MorphoSource DOI: [10.17602/M2/M432529](#)

639   - 17 Penises of *Xenos vesparum* surface models

640   pmj:Strep_43/02: Media 000432535; MorphoSource DOI: [10.17602/M2/M432535](#)

641   pmj:Strep_43/03: Media 000432541; MorphoSource DOI: [10.17602/M2/M432541](#)

642   pmj:Strep_43/04: Media 000432547; MorphoSource DOI: [10.17602/M2/M432547](#)

643   pmj:Strep_43/05: Media 000432553; MorphoSource DOI: [10.17602/M2/M432553](#)

644 pmj:Strep_43/06: Media 000432559; MorphoSource DOI: [10.17602/M2/M432559](10.17602/M2/M432559)

645 pmj:Strep_43/07: Media 000432565; MorphoSource DOI: [10.17602/M2/M432565](10.17602/M2/M432565)

646 pmj:Strep_43/08: Media 000432571; MorphoSource DOI: [10.17602/M2/M432571](10.17602/M2/M432571)

647 pmj:Strep_43/09: Media 000432577; MorphoSource DOI: [10.17602/M2/M432577](10.17602/M2/M432577)

648 pmj:Strep_43/10: Media 000432583; MorphoSource DOI: [10.17602/M2/M432583](10.17602/M2/M432583)

649 pmj:Strep_43/11: Media 000432589; MorphoSource DOI: [10.17602/M2/M432589](10.17602/M2/M432589)

650 pmj:Strep_43/12: Media 000432595; MorphoSource DOI: [10.17602/M2/M432595](10.17602/M2/M432595)

651 pmj:Strep_43/13: Media 000432601; MorphoSource DOI: [10.17602/M2/M432601](10.17602/M2/M432601)

652 pmj:Strep_43/14: Media 000432607; MorphoSource DOI: [10.17602/M2/M432607](10.17602/M2/M432607)

653 pmj:Strep_43/15: Media 000432613; MorphoSource DOI: [10.17602/M2/M432613](10.17602/M2/M432613)

654 pmj:Strep_43/16: Media 000432619; MorphoSource DOI: [10.17602/M2/M432619](10.17602/M2/M432619)

655 pmj:Strep_43/17: Media 000432625; MorphoSource DOI: [10.17602/M2/M432625](10.17602/M2/M432625)

656 pmj:Strep_43/18: Media 000432631; MorphoSource DOI: [10.17602/M2/M432631](10.17602/M2/M432631)

657 **References**

658 **Adams DC, Collyer ML, Kaliontzopoulou A, Sherratt E**. **2021.** Geomorph: Software for

659   geometric morphometric analyses. R package version 4.0.2.

660 **Arnqvist G, Rowe L**. **2002.** Antagonistic coevolution between the sexes in a group of insects.

661   *Nature* **415**:787–789.

662 **Baer B, Boomsma JJ**. **2006.** Mating biology of the leaf-cutting ants *Atta colombica* and *A.*

663   *cephalotes*. *Journal of Morphology* **267**:1165–1171.

664 **Baken EK, Collyer ML, Kaliontzopoulou A, Adams DC**. **2021.** geomorph v4. 0 and gmShiny:

665   Enhanced analytics and a new graphical interface for a comprehensive morphometric

666   experience. *Methods in Ecology and Evolution* **12**:2355–2363.

667 **Beani L, Giusti F, Mercati D, Lupetti P, Paccagnini E, Turillazzi S, Dallai R. 2005.** Mating

668   of *Xenos vesparum* (Rossi) (Strepsiptera, Insecta) revisited. *Journal of Morphology*

669   **265**:291–303.

670 **Beani L, Cappa F, Manfredini F, Zaccaroni M. 2018.** Preference of *Polistes dominula* wasps

671   for trumpet creepers when infected by *Xenos vesparum*: A novel example of co-evolved

672   traits between host and parasite. *PloS one* **13**.

673 **Benda D, Pohl H, Nakase Y, Beutel RG, Straka J**. **2022.** A generic classification of Xenidae

674   (Strepsiptera) based on the morphology of the female cephalothorax and male

675   cephalotheca with a preliminary checklist of species. *ZooKeys* **1093**:1–134.

676 **Brand JN, Harmon LJ, Schaerer L**. **2022.** Frequent origins of traumatic insemination involve

677   convergent shifts in sperm and genital morphology. *Evolution Letters* **6**:63–82.

678 **Cecilia A, Rack A, Douissard P-A, Martin T, dos Santos Rolo T, Vagovič P, Hamann E,**

679   **van de Kamp T, Riedel A, Fiederle M**. **2011.** LPE grown LSO: Tb scintillator films for

680 high-resolution X-ray imaging applications at synchrotron light sources. *Nuclear*

681 *Instruments and Methods in Physics Research Section A: Accelerators, Spectrometers,*

682 *Detectors and Associated Equipment* **648**:321–323.

683 **Cook JL, Mayorga-Ch D, Sarmiento CE**. **2020.** A new species of *Xenos* (Strepsiptera:

684 Xenidae) from Colombia, with comments on the Neotropical species of the genus.

685 *Transactions of the American Entomological Society* **146**:331–339.

686 **Dallai R, Lupetti P, Giusti F, Mercati D, Paccagnini E, Turillazzi S, Beani L,**

687 **Kathirithamby J. 2004.** Fine structure of the Nassonow's gland in the neotenic

688 endoparasitic of female *Xenos vesparum* (Rossi) (Strepsiptera, Insecta). *Tissue and Cell*

689 **36**:211–220

690 **Dougherty LR, Simmons LW**. **2017.** X-ray micro-CT scanning reveals temporal separation of

691 male harm and female kicking during traumatic mating in seed beetles. *Proceedings of*

692 *the Royal Society B: Biological Sciences* **284**.

693 **Douissard P-A, Cecilia A, Rochet X, Chapel X, Martin T, van de Kamp T, Helfen L,**

694 **Baumbach T, Luquot L, Xiao X**. **2012.** A versatile indirect detector design for hard X-

695 ray microimaging. *Journal of Instrumentation* **7**:P09016.

696 **Eberhard WG**. **2004a.** Male–female conflict and genitalia: failure to confirm predictions in

697 insects and spiders. *Biological Reviews* **79**:121–186.

698 **Eberhard WG**. **2004b.** Rapid divergent evolution of sexual morphology: comparative tests of

699 antagonistic coevolution and traditional female choice. *Evolution* **58**:1947–1970.

700 **Faragó T, Mikulík P, Ershov A, Vogelgesang M, Hänschke D, Baumbach T**. **2017.** Syris: a

701 flexible and efficient framework for X-ray imaging experiments simulation. *Journal of*

702 *synchrotron radiation* **24**:1283–1295.

703 **Folmer O, Black M, Hoeh W, Lutz R, Vrijenhoek R**. **1994.** DNA primers for amplification of

704   mitochondrial cytochrome c oxidase subunit I from diverse metazoan invertebrates.

705   *Molecular Marine Biology and Biotechnology* **3**:294–299.

706 **Grabert B. 1953.** *Bau der Geschlechtsorgane und Kopulation beim* Stylops-*Männchen (Insecta,*

707   *Strepsiptera)*. Berlin: Freie Universität Berlin.

708 **Hughes D, Kathirithamby J, Turillazzi S, Beani L 2004.** Social wasps desert the colony and

709   aggregate outside if parasitized: parasite manipulation? *Behavioral Ecology* **15**:1037–

710   1043.

711 **Jůzová K, Nakase Y, Straka J**. **2015.** Host specialization and species diversity in the genus

712   *Stylops* (Strepsiptera: Stylopidae), revealed by molecular phylogenetic analysis.

713   *Zoological Journal of the Linnean Society* **174**:228–243.

714 **Kamimura Y**. **2007.** Twin intromittent organs of *Drosophila* for traumatic insemination.

715   *Biological Letters* **3**:401–404.

716 **Kathirithamby J, Hrabar M, Delgado JA, Collantes F, Dötterl S, Windsor D, Gries G**.

717   **2015.** We do not select, nor are we choosy: reproductive biology of Strepsiptera (Insecta).

718   *Biological Journal of the Linnean Society* **116**:221–238.

719 **Kathirithamby J, Hughes DP**. **2006.** Description and biological notes of the first species of

720   *Xenos* (Strepsiptera: Stylopidae) parasitic in *Polistes carnifex* F.(Hymenoptera: Vespidae)

721   in Mexico. *Zootaxa* **1104**:35–45.

722 **Kifune T**. **1986.** A new species of the genus *Xenos* (Strepsiptera, Stylopidae) parasitic on the

723   genus *Provespa* (Hymenoptera, Vespidae) from West Sumatra, Indonesia (Notulae

724   Strepsipterologicae XVI). *Kontyû* **54**:84–88.

725   **Kifune T, Maeta Y**. **1975.** A new subgenus and new species of the genus *Xenos* (Strepsiptera,

726   Stylopidae) from Japan. (studies on the Japanese Strepsiptera III). *Kontyû* **43**:446–455.

727   **Kifune T, Maeta Y**. **1985.** Taxonomical studies on the genus *Xenos* (Strepsiptera, Stylopidae)

728   parasitic on *Vespa* and *Polistes (*Hymenoptera, Vespidae) of Taiwan with descriptions of

729   three new species (Notulae Strepsipterologicae XIV). *Kontyû* **53**:426–435.

730   **Kinzelbach R. 1971.** *Morphologische Befunde an Fächerflüglern und ihre phylogenetische*

731   *Bedeutung (Insecta: Strepsiptera).* Stuttgart: Zoologica. E. Schweizerbart'sche

732   Verlagsbuchhandlung (Nägele u. Obermiller).

733   **Kinzelbach RK. 1978.** *Fächerflügler (Strepsiptera), Die Tierwelt Deutschlands.* Jena: VEB

734   Gustav Fischer Verlag.

735   **Lagoutte R, Šebesta P, Jiroš P, Kalinová B, Jirošová A, Straka J, Černá K, Šobotník J,**

736   **Cvačka J, Jahn U**. **2013.** Total synthesis, proof of absolute configuration, and

737   biosynthetic origin of stylopsal, the first isolated sex pheromone of Strepsiptera.

738   *Chemistry – A European Journal* **19**:8515–8524.

739   **Lange R, Reinhardt K, Michiels NK, Anthes N**. **2013.** Functions, diversity, and evolution of

740   traumatic mating. *Biological Reviews* **88**:585–601.

741   **Lauterbach G**. **1954.** Begattung und Larvengeburt bei den Strepsipteren. *Zeitschrift für*

742   *Parasitenkunde* **16**:255–297.

743   **Löwe S, Beutel RG, Pohl H**. **2016.** The female cephalothorax of *Stylops ovinae* Noskiewicz &

744   Poluszyński, 1928 (Strepsiptera: Stylopidae). *Arthropod Systematics & Phylogeny* **74**:65–

745   81.

746 **Matsumura Y, Suenaga H, Kamimura Y, Gorb SN**. **2017.** Traumatic mating by hand saw-like

747   spines on the internal sac in *Pyrrhalta maculicollis* (Coleoptera, Chrysomelidae,

748   Galerucinae). *ZooKeys* **720**:77–89.

749 **McMahon DP, Hayward A, Kathirithamby J**. **2009.** The mitochondrial genome of the

750   'twisted-wing parasite' *Mengenilla australiensis* (Insecta, Strepsiptera): a comparative

751   study. *BMC Genomics* **10**:1–15.

752 **Merritt DJ**. **1989.** The morphology of the phallosome and accessory gland material transfer

753   during copulation in the blowfly, *Lucilia cuprina* (Insecta, Diptera). *Zoomorphology*

754   **108**:359–366.

755 **Michels J, Büntzow M**. **2010.** Assessment of Congo red as a fluorescence marker for the

756   exoskeleton of small crustaceans and the cuticle of polychaetes. *Journal of Microscopy*

757   **238**:95–101.

758 **Michels J, Gorb SN**. **2012.** Detailed three-dimensional visualization of resilin in the exoskeleton

759   of arthropods using confocal laser scanning microscopy. *Journal of Microscopy* **245**:1–

760   16.

761 **Michels J, Gorb SN, Reinhardt K**. **2015.** Reduction of female copulatory damage by resilin

762   represents evidence for tolerance in sexual conflict. *Journal of the Royal Society*

763   *Interface* **12**:20141107.

764 **Nakase Y, Kato M**. **2013.** Cryptic diversity and host specificity in giant *Xenos* strepsipterans

765   parasitic in large *Vespa* hornets. *Zoological Science*:331–336.

766 **Paganin D, Mayo SC, Gureyev TE, Miller PR, Wilkins SW**. **2002.** Simultaneous phase and

767   amplitude extraction from a single defocused image of a homogeneous object. *Journal of*

768   *Microscopy* **206**:33–40.

769   **Parker GA**. **2006.** Sexual conflict over mating and fertilization: an overview. *Philosophical*

770   *Transactions of the Royal Society B: Biological Sciences* **361**:235–259.

771   **Peinert M, Wipfler B, Jetschke G, Kleinteich T, Gorb SN, Beutel RG, Pohl H**. **2016.**

772   Traumatic insemination and female counter-adaptation in Strepsiptera (Insecta). *Scientific*

773   *Reports* **6**:25052.

774   **Pohl H**. **2010.** A scanning electron microscopy specimen holder for viewing different angles of a

775   single specimen. *Microscopy Research and Technique* **73**:1073–1076.

776   **Pohl H, Beutel RG**. **2008.** The evolution of Strepsiptera (Hexapoda). *Zoology* **111**:318–338.

777   **Reinhardt K, Anthes N, Lange R**. **2015.** Copulatory wounding and traumatic insemination.

778   *Cold Spring Harbor perspectives in biology* **7**:a017582.

779   **Richter A, Wipfler B, Beutel RG, Pohl H**. **2017.** The female cephalothorax of *Xenos vesparum*

780   Rossi, 1793 (Strepsiptera: Xenidae). *Arthropod Structure & Development* **75**:327–347.

781   **Rönn J, Katvala M, Arnqvist G**. **2007.** Coevolution between harmful male genitalia and female

782   resistance in seed beetles. *Proceedings of the National Academy of Sciences* **104**:10921–

783   10925.

784   **Straka J, Jůzová K, Nakase Y**. **2015.** Nomenclature and taxonomy of the genus *Stylops*

785   (Strepsiptera): an annotated preliminary world checklist. *Acta Entomologica Musei*

786   *Nationalis Pragae* **55**:305–332.

787   **Tatarnic NJ, Cassis G, Siva-Jothy MT**. **2014.** Traumatic insemination in terrestrial arthropods.

788   *Annual Review of Entomology* **59**:245–261.

789   **Tolasch T, Kehl S, Dötterl S**. **2012.** First sex pheromone of the order Strepsiptera:(3 R, 5 R, 9

790   R)-3, 5, 9-Trimethyldodecanal in *Stylops melittae* Kirby, 1802. *Journal of Chemical*

791   *Ecology* **38**:1493–1503.

792 **Vogelgesang M, Chilingaryan S, dos Santos Rolo T, Kopmann A.** 2012. UFO: a scalable

793   GPU-based image processing framework for on-line monitoring. 2012 IEEE 14th

794   International Conference on High Performance Computing and Communications & 2012

795   IEEE 9th International Conference on Embedded Software and Systems: IEEE. p 824–

796   829.

797 **Vogelgesang M, Farago T, Morgeneyer TF, Helfen L, dos Santos Rolo T, Myagotin A,**

798   **Baumbach T**. **2016.** Real-time image-content-based beamline control for smart 4D X-ray

799   imaging. *Journal of Synchrotron Radiation* **23**:1254–1263.

Figure 1

Photographs of *Stylops ovinae* and *Xenos vesparum.*

(A) Frontal view of an adult male *S. ovinae.* (B) One female of *S. ovinae* protrudes from its host's metasoma (*Andrena vaga)*. (C) Frontal view of an adult male *X. vesparum.* (D) Two females of *X. vesparum* protruding from their host's metasoma (*Polistes dominula*). Arrowheads indicate strepsipteran females.
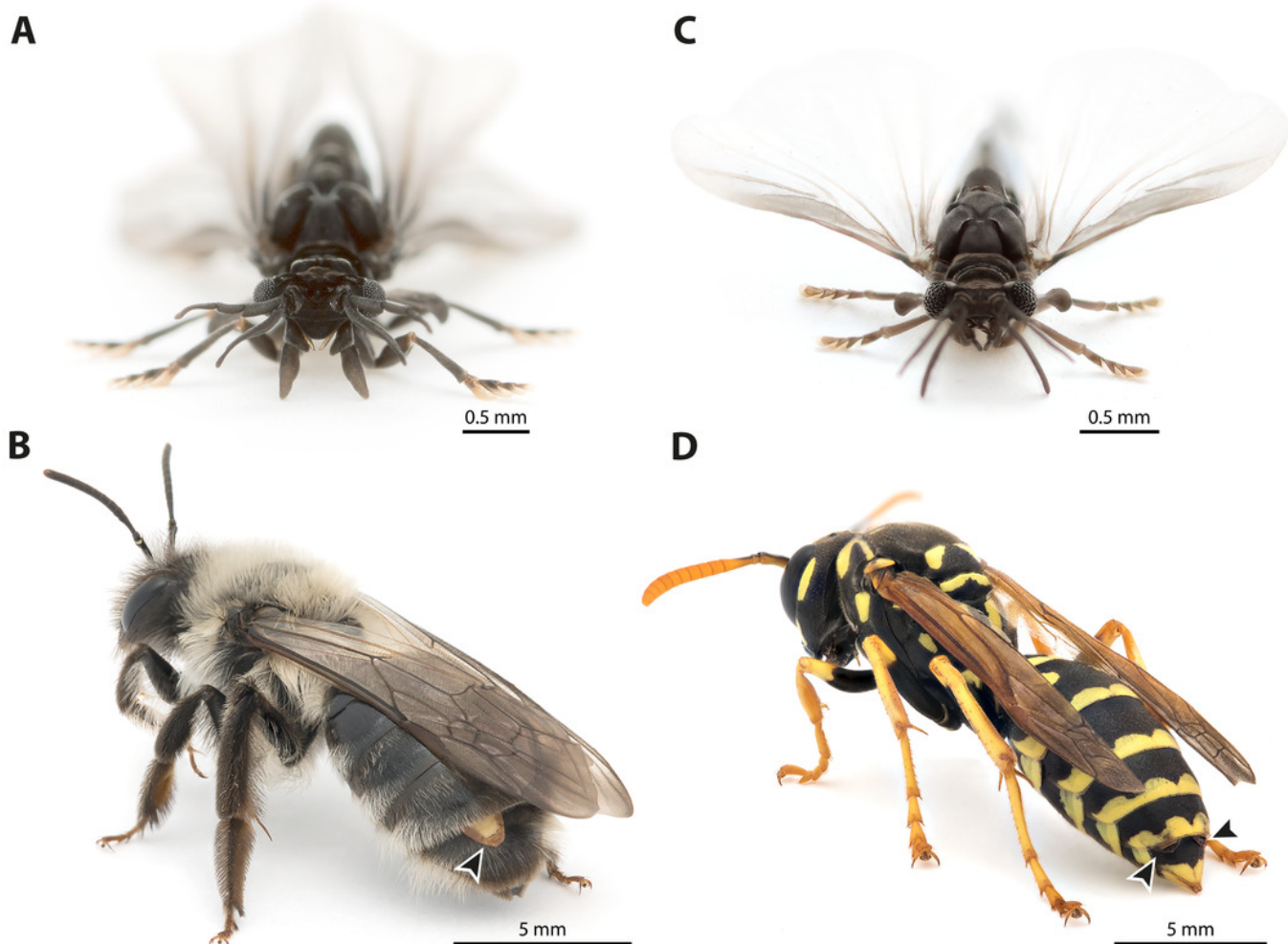
Figure 2

Sagittal sections of female cephalothoraces of *Stylops ovinae* (A) and *Xenos vesparum* (B).

Abbreviations: bc – brood canal, bo – birth opening, ct – cuticle, ed – epidermis, ex2 – exuvia of the secondary larval stage, ng – Nassonow's gland, po – paragenital organ, ws – wounding site, cs – control site. (A) Modified from *Peinert et al. (2016)*. (B) Modified from *Richter et al. (2017)*.

A

ct ed bc cs ng

bo

ex2 po

ws

200 μm

B

ws ct ed bc ex2 cs ng

bo

200 μm
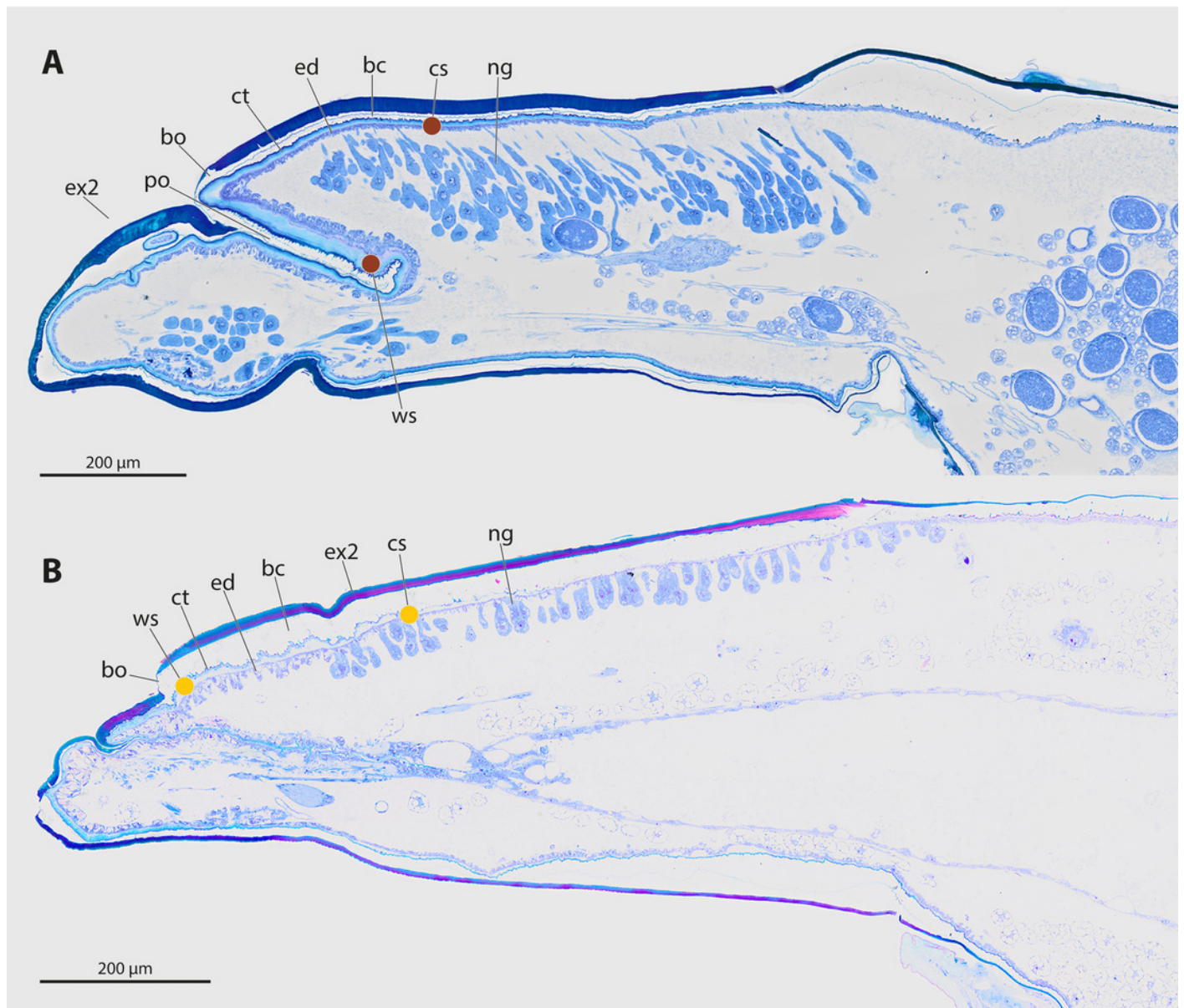
Figure 3

Female cephalothoraces of *Stylops ovinae* (A) and *Xenos vesparum* (B) with mating signs (outer cuticle of the cephalothorax removed).

Abbreviation: ms – mating sign. (A) modified from (*Peinert et al., 2016*).
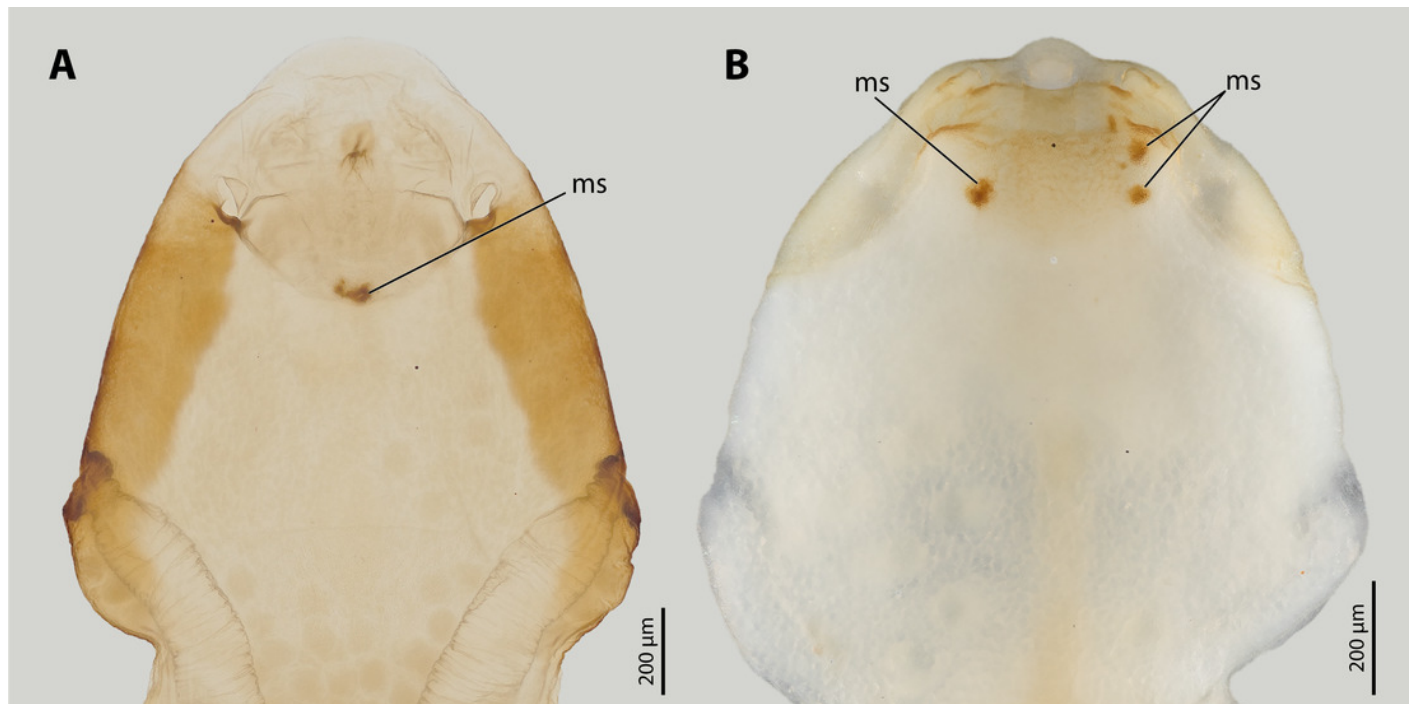
Figure 4

Penises of different species of *Stylops* (red) and *Xenos* (yellow).

(A) *S. ovinae*. (B) *S. hammella*. (C) *S. liliputanus*. (D) *S. aterrimus*. (E) *S. melittae*. (F) *X. columbiensis*. (G) *X. moutoni*. (H) *X. oxydontes*. (I) *X. vesparum*. B–E modified after *Kinzelbach (1978)*, F modified after *Cook, Mayorga-Ch & Sarmiento (2020)*, G modified after *Kifune & Maeta (1985)*, H modified after *Nakase & Kato (2013)*.
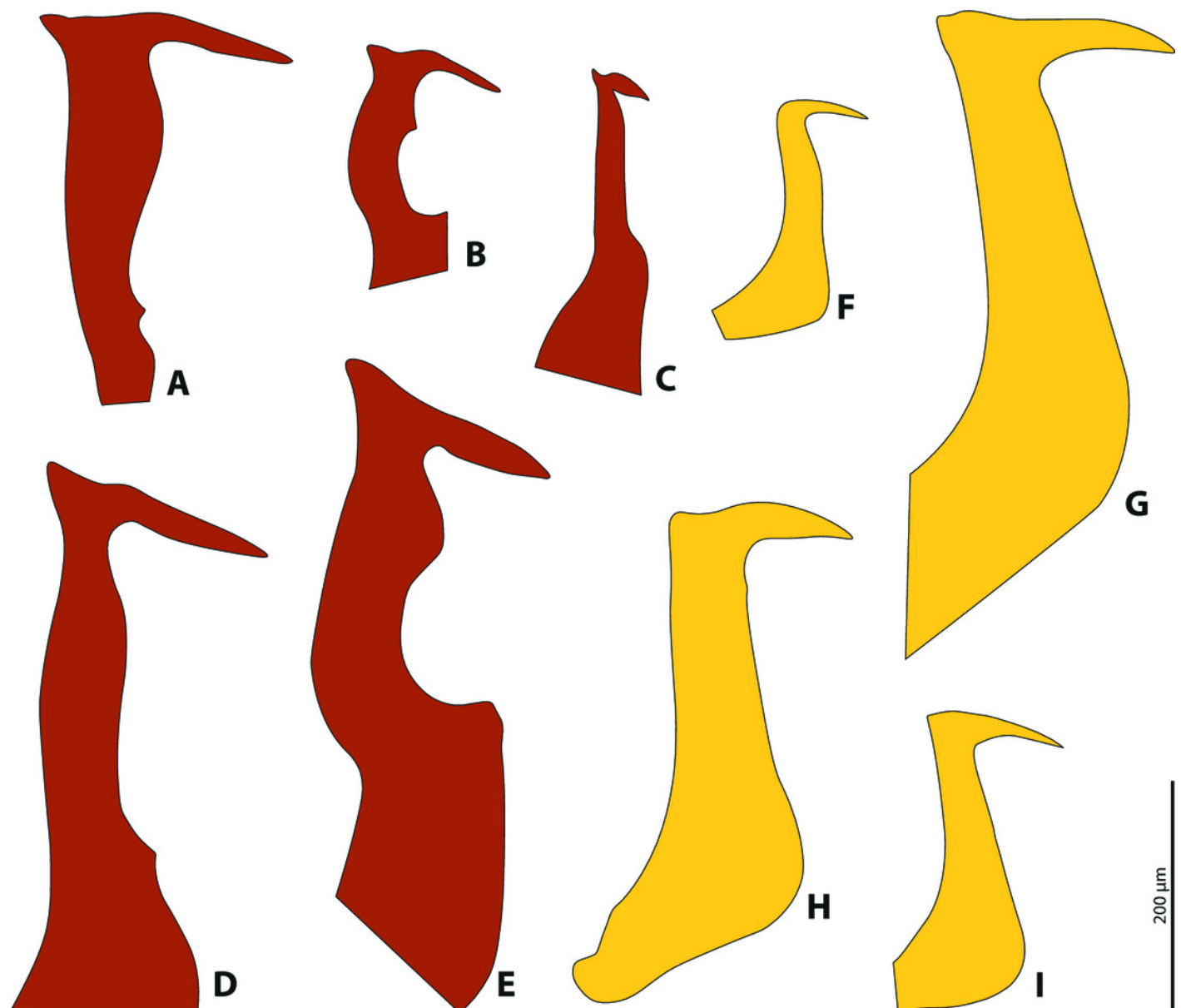
Figure 5

Confocal laser scanning micrographs (maximum intensity projections) showing the cuticle autofluorescence composition of female *Stylops ovinae* and *Xenos vesparum* cephalothoraces (outer cuticle of the cephalothorax removed).

(A) Morphological ventral side of *S. ovinae*. (B) Morphological ventral side of *X. vesparum*.

Blue structures contain large proportions of the elastomeric protein resilin. Green structures

are chitinous and membranous and either weakly-sclerotised or non-sclerotised.

Abbreviations: cs – control site, po – paragenital organ, ws – wounding site.
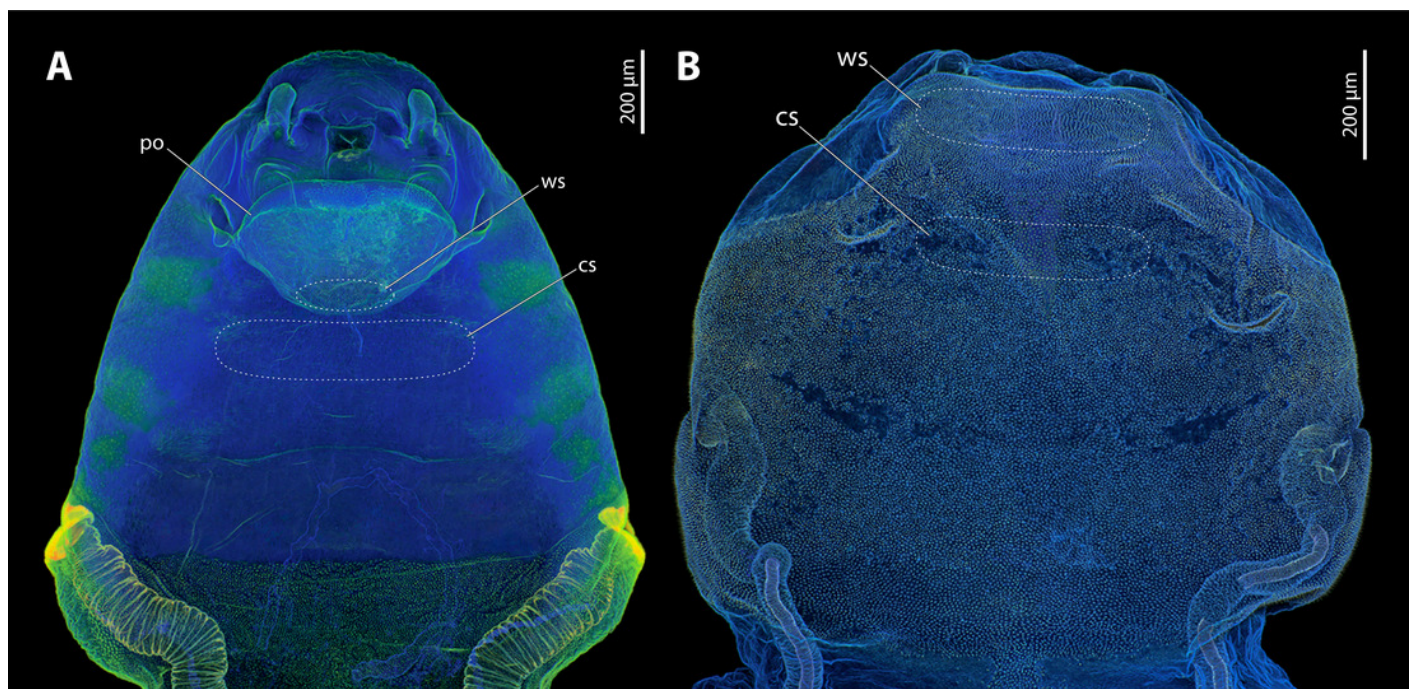
Figure 6

Critical stress values for wounding and control sites of *Stylops ovinae* (red) and *Xenos vesparum* (yellow).

Stylops ovinae: wounding site – ventral wall of the paragenital organ, control site – anterior brood canal. **Xenos vesparum**: wounding site – anterior brood canal; control site – posterior brood canal. Boxes represent the interquartile range between first and third quartiles, and the line inside represents the median. Whiskers denote the lowest and highest values within 1.5× interquartile range from the first and third quartiles, respectively. Circles represent outliers beyond the whiskers.
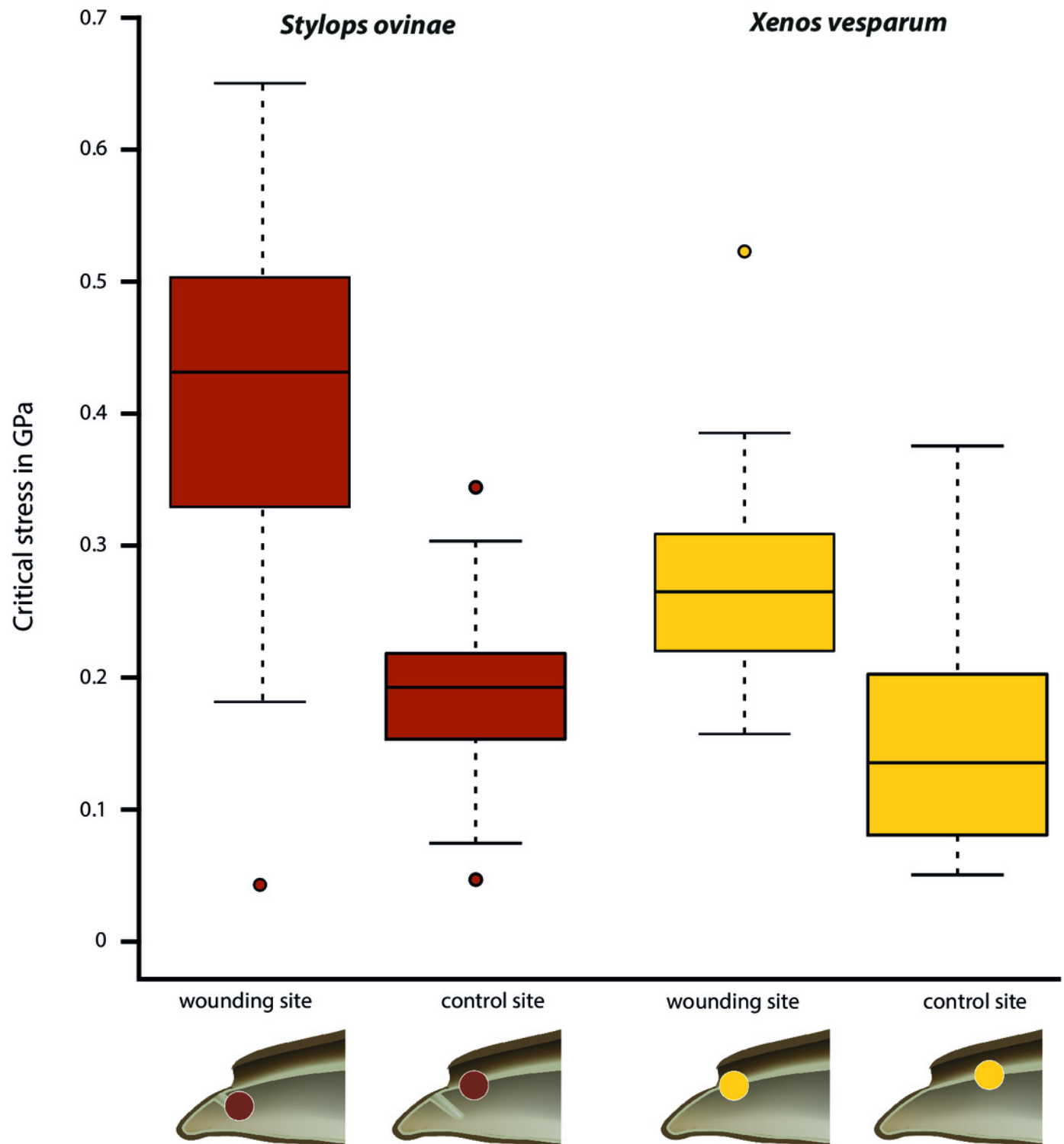
Figure 7

Pairs of female cephalothoraces (outer cuticle of the cephalothorax removed) and male penises of *Stylops hammella*(A), *Stylops ovinae* (B) and *Stylops melittae* (C).

Paragenital organs highlighted in ochre, penises in red. *S. ovinae* was scanned in copula (*Peinert et al., 2016*). The penises of *S. hammella* and *S. melittae* were virtually inserted into the corresponding conspecific female paragenital organs to assess the fit of these genital structures.
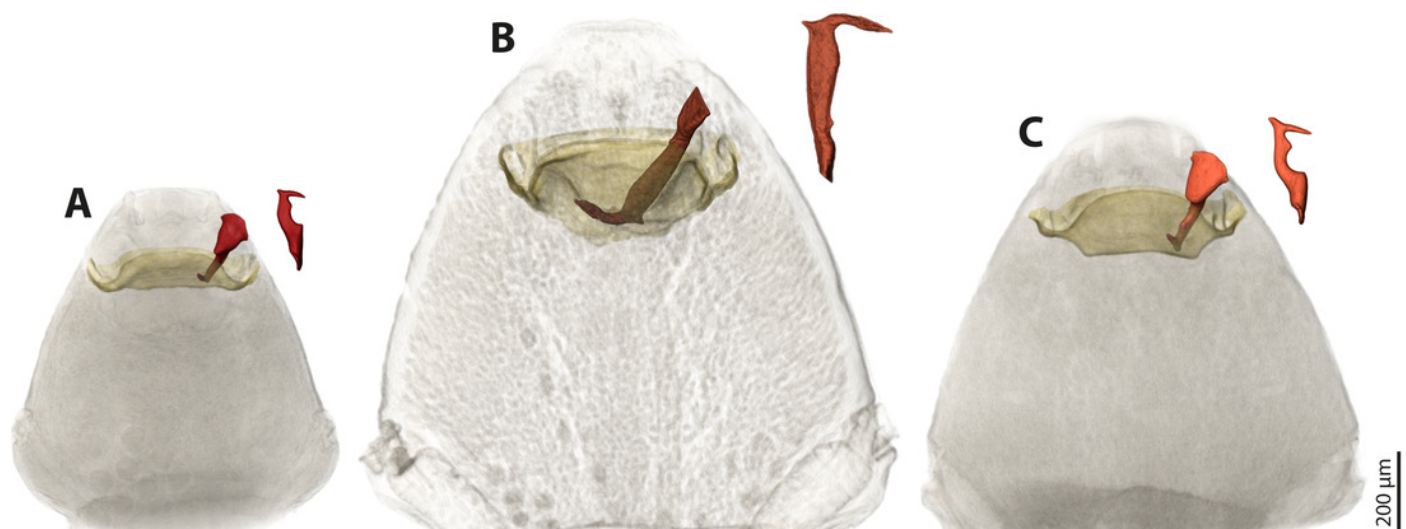
Figure 8

Geometric morphometric analysis of penises of *Stylops ovinae* (red) and *Xenos vesparum* (yellow).

(A) Lateral view of all investigated penises of both species. (B) Shape spaces of penises of both species visualised with the three most representative principal components (see supplementary for interactive 3D version). (C) and (D) Shape change along the PC axes of *S. ovinae* (C) and *X. vesparum* (D). Darker colours represent lower PC values, while brighter colours outline higher PC values.
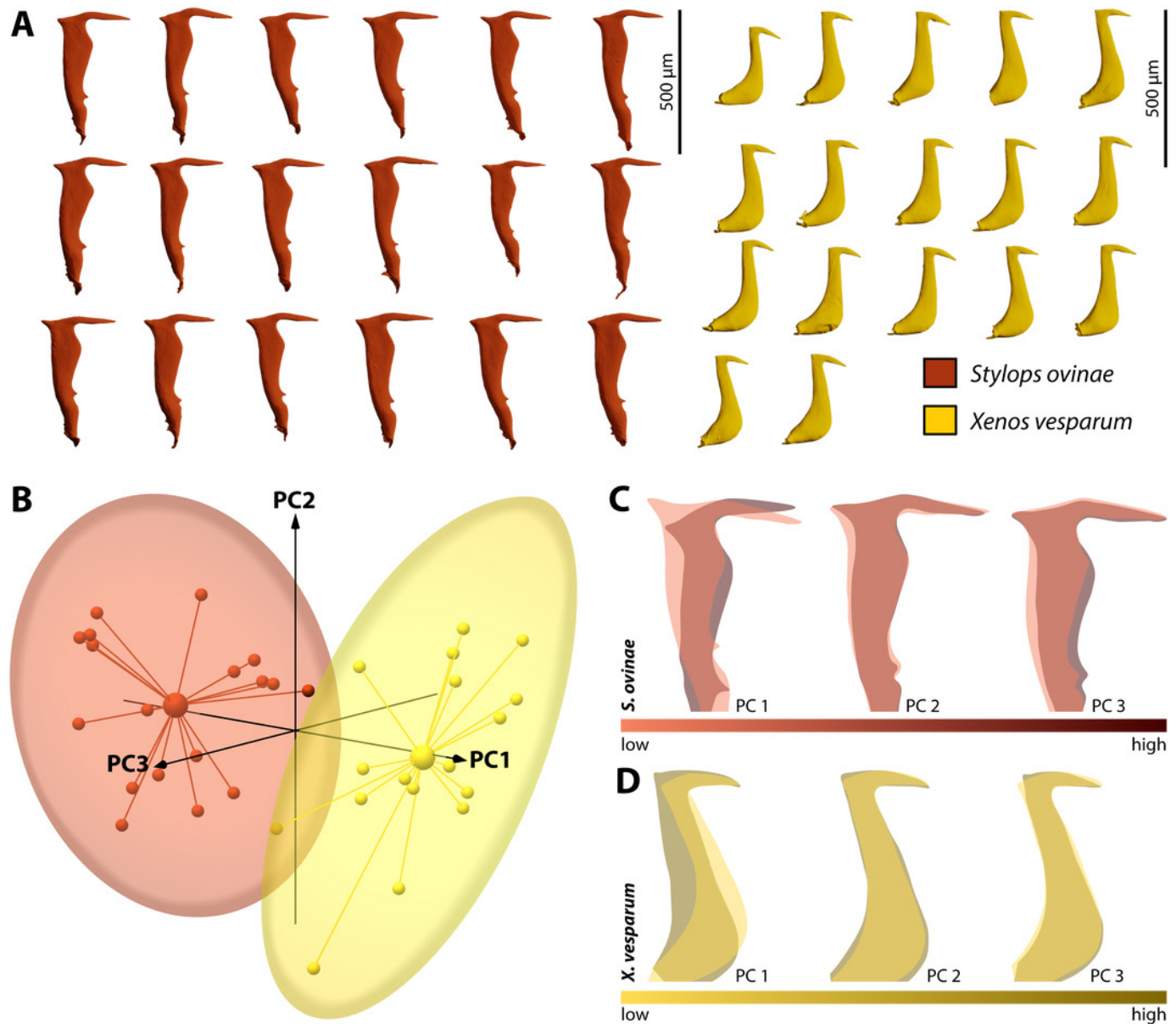
Means, standard deviations (SD) and *p* values from Shapiro-Wilk tests (SWT).

Abbreviation: mN – millinewton; GPa – gigapascal.

	Penetration force			Critical stress		
	Mean (mN)	**SD**	**SWT**	**Mean** GPa	**SD**	**SWT**
S. ovinae (wounding site) n = 30	9.723	3.498	0.09288335	0.402	0.138	0.09427896
S. ovinae (control site) n = 40	4.578	1.483	0.7888944	0.186	0.060	0.7888944
X. vesparum (wounding site) n = 38	3.669	1.011	0.03403307	0.273	0.075	0.03404492
X. vesparum (control site) n = 36	2.003	1.077	0.01891762	0.149	0.080	0.01892339

Results of the Wilcoxon pairwise comparison of means for the penetration force and the critical stress of female *Stylops ovinae* and *Xenos vesparum*.

p, probability value; *, indicates significance.

Penetration force	*S. ovinae* (wounding site)	*S. ovinae* (control site)	*X. vesparum* (wounding site)
S. ovinae (control site)	p =2.1e-08*	−	−
X. vesparum (wounding site)	p = 2.8e-11*	p = 0.00159*	−
X. vesparum (control site)	p = 1.6e-13*	p = 5.5e-11*	p = 1.5e-08*
Critical stress			−
S. ovinae (control site)	p = 7.5e-09*	−	−
X. vesparum (wounding site)	p = 4.1e-05*	p = 1.2e-06*	−
X. vesparum (control site)	p = 1.7e-09*	p = 0.0327*	p = 2.7e-08*